PERGAMON

International Journal of Heat and Mass Transfer 42 (1999) 2837–2847

International Journal of HEAT and MASS TRANSFER

Momentum and heat transfer in a power-law fluid with arbitrary injection/suction at a moving wall

J.H. Rao[a], D.R. Jeng[b,*], K.J. De Witt[a]

[a] *Department of Chemical Engineering, College of Engineering, The University of Toledo, Toledo, OH 43606, U.S.A.*
[b] *Department of Mechanical Engineering, College of Engineering, The University of Toledo, Toledo, OH 43606, U.S.A.*

Received 27 January 1998; in final form 20 October 1998

Abstract

The momentum and heat transfer in the laminar boundary layer of a non-Newtonian power-law fluid flowing over a flat plate, which is moving in the direction opposite to the uniform main stream, and with arbitrary fluid injection/suction along the plate surface, are analyzed. The partial differential equations are decomposed into a sequence of ordinary differential equations using the Merk–Chao series to obtain universal velocity and temperature functions that are independent of the fluid injection/suction distribution profile. Results are tabulated as a function of the problem parameters. Friction coefficients and Nusselt numbers are calculated for constant fluid injection/suction along the plate.

Nomenclature

c_f friction coefficient defined by equation (40)
$\hat{C}_p$ specific heat at constant pressure
f dimensionless stream function defined in equation (10)
k thermal conductivity
L reference length
n power-law exponent defined in equation (4)
Nu Nusselt number defined in equation (42)
Pr generalized Prandtl number defined in equation (30)
Re generalized Reynolds number defined in equation (9)
T temperature
u fluid velocity component in x-direction
U_w plate velocity in the negative x-direction
U_∞ main stream velocity
v fluid velocity component in y-direction
v_0 constant injection velocity at the wall
$V_w(x)$ injection velocity at the plate surface
$V(\xi)$ dimensionless injection distribution defined in equation (13)
x stream wise coordinate along surface measured from the slot
y coordinate normal to plate surface.

Greek symbols

α thermal diffusivity
η dimensionless variable defined in equation (8b)
θ dimensionless temperature defined in equation (26)
λ plate velocity ratio defined in equation (17a)
Λ injection parameter defined by equation (16)
Λ_1 parameter in the energy equation defined by equation (29)
μ_0 consistency index for non-Newtonian viscosity defined in equation (4)
ξ dimensionless variable defined in equation (8a)
ρ density
τ_{yx} shear stress defined in equation (4)
ψ stream function defined in equations (7a,b).

Subscripts

i subscript designating universal functions
w subscript designating the conditions at the plate surface
∞ subscript designating the conditions in the main stream.

* Corresponding author. Tel.: 001 419 530 8223; fax: 001 419 530 8206; e-mail: djeng@uofto2.utoledo.edu

0017–9310/99/$ - see front matter
PII: S0017–9310(98)00360–3

1. Introduction

A majority of non-Newtonian fluids fall into the time-independent classification, which includes power-law fluids. Power-law fluids, which have been called Ostwald-de-Waele fluids by some authors, have been well examined because the constitutive equation for such a fluid not only gives a good expression for a large portion of non-Newtonian fluids but also encompasses a Newtonian fluid as well. For a non-Newtonian fluid, the viscous stress is a nonlinear function of the rate of deformation, and the relationship for the power-law fluid is given by equation (4) in the next section.

The theoretical problem of external, boundary layer flow of a non-Newtonian fluid was first investigated by Schowalter [1], who formulated the boundary layer equations and established the conditions for the existence of a similarity solution. Acrivos et al. [2] obtained a similarity solution for a power-law fluid flowing over a flat plate at zero degree incidence. Later, generalized studies on the question of similar solutions for non-Newtonian fluids and the types of inviscid flow fields consistent with the concept of similarity were done by Lee and Ames [3], Berkovskii [4] and Hansen and Na [5].

All of the above studies were done for the case of impermeable walls. The experimental results that significant drag reduction can be achieved by injecting fluid into the boundary layer [6] motivated the investigations of non-Newtonian boundary layer flows with injection at the surface. The effect of wall mass injection on the flow of a non-Newtonian power-law fluid over a flat plate was first investigated by Thompson and Snyder [7, 8]. The solutions for stagnation flow and wedge flow were obtained by Kim and Eraslan [9, 10]. Liu [11] presented a class of asymptotic suction solutions for the flow of power-law fluids over a flat plate.

Klemp and Acrivos [12] studied the problem in which a flat plate moves in the direction opposite to the mainstream. Hussaini and Lakin [13] showed that a boundary layer solution to such a problem exists only if the ratio of the plate velocity to the main stream velocity is below a critical value. Vajravelu and Mohapatra [14] extended this analysis to the case where there is mass injection at the wall and proved that for a given value of plate velocity there exists a critical value of injection beyond which the boundary layer approximations are no longer applicable.

In all of the works on boundary layer suction or injection mentioned so far, the major emphasis has been to obtain a similarity solution. The similarity solution, however, exists for only one particular fluid injection distribution. The current work presents a method for obtaining the general boundary layer solution for any fluid injection/suction profile along the moving flat plate, and contains the similarity solution as a special case.

2. Formulation of governing equations

Consider an incompressible, power-law fluid flowing over a porous flat plate in a stationary coordinate system, as shown in Fig. 1. The velocity and the temperature of the uniform main stream are U_∞ and T_∞, respectively. The plate is moving in the negative x-direction into a slot at the origin with a velocity U_w. At the surface of the plate, which is maintained at a uniform temperature T_w, the same fluid is being injected/sucked with a velocity $V_w(x)$. It is assumed that all physical properties of the fluid are constant and that the magnitude of the injection velocity is not large enough to significantly alter the inviscid flow field outside the boundary layer. With these assumptions, the steady state boundary layer equations for a flat plate are:

$$\text{Continuity} \quad \frac{\partial u}{\partial x}+\frac{\partial v}{\partial y}=0. \tag{1}$$

$$\text{Momentum} \quad u\frac{\partial u}{\partial x}+v\frac{\partial u}{\partial y}=\frac{1}{\rho}\frac{\partial}{\partial y}(\tau_{yx}) \tag{2}$$

with the boundary conditions:

$$u=-U_w, \quad v=V_w(x) \quad \text{at } y=0 \tag{3a,b}$$

$$u=U_\infty \quad \text{at } y=\infty. \tag{3c}$$

For power-law fluids the shear stress is given by

$$\tau_{yx}=\mu_0\left|\frac{\partial u}{\partial y}\right|^{n-1}\frac{\partial u}{\partial y} \tag{4}$$

where μ_0 and n are called the consistency index and the power-law exponent, respectively. In equation (4), the quantity μ_0 is not the viscosity in a classical sense unless n is unity. The parameter n is an important index to subdivide fluids into pseudo-plastic fluids ($n<1$) and dilatant fluids ($n>1$). Pseudo-plastic fluids are more frequently encountered in the physical world than dilatant fluids. Since the velocity in the x-direction is continuously increasing along the y-direction, $\partial u/\partial y$ is always positive

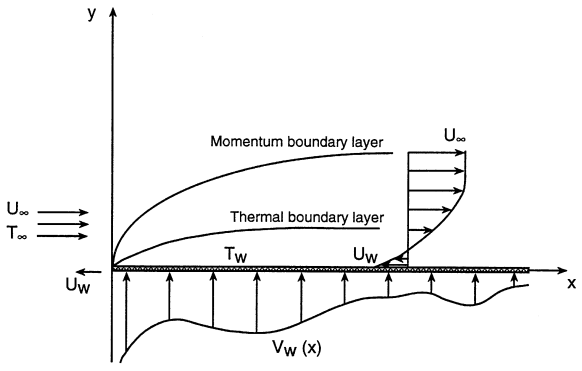

Fig. 1. Schematic representation of momentum and thermal boundary layers.

and one can remove the absolute value sign in equation (4).

$$\text{Thermal energy equation} \quad u\frac{\partial T}{\partial x}+v\frac{\partial T}{\partial y}=\alpha\frac{\partial^2 T}{\partial y^2} \tag{5}$$

with the boundary conditions:

$$T=T_w \quad \text{at } y=0 \tag{6a}$$

$$T=T_\infty \quad \text{at } y=\infty. \tag{6b}$$

Since the momentum and the energy equations are not coupled, the solution to the momentum equation can be discussed first.

3. Solution of the momentum equation

A stream function is introduced to satisfy the continuity equation and to make the right-hand-side of the boundary condition (3b) a constant:

$$u=\frac{1}{L}\frac{\partial\psi}{\partial y}, \quad v=-\frac{1}{L}\frac{\partial\psi}{\partial x}+V_w(x). \tag{7a,b}$$

Also, the following dimensionless variables are introduced:

$$\xi=\frac{n}{Re}\left(\frac{x}{L}\right), \quad \eta=[(n+1)\xi]^{(-1)/(n+1)}\left(\frac{y}{L}\right) \tag{8a,b}$$

where

$$Re=\frac{\rho U_\infty^{2-n}L^n}{\mu_0} \tag{9}$$

is the generalized Reynolds number. The stream function is also non-dimensionalised by defining

$$\psi=[(n+1)\xi]^{1/(n+1)}U_\infty L^2 f(\xi,\eta). \tag{10}$$

In terms of the new variables, the fluid velocity components are

$$u=U_\infty\frac{\partial f}{\partial\eta} \tag{11}$$

$$v=-nU_\infty Re^{-1}[(1+1)\xi]^{(-n)/(n+1)}\left\{f+\xi(n+1)\frac{\partial f}{\partial\xi}-\eta\frac{\partial f}{\partial\eta}\right\}+V(\xi) \tag{12}$$

where

$$V(\xi)=V_w\left(\frac{Re\,L}{n}\xi\right). \tag{13}$$

The momentum equation (2) is transformed to

$$f'''f''^{(n-1)}+(f-\Lambda)f''=(n+1)\xi\frac{\partial(f',f)}{\partial(\xi,\eta)} \tag{14}$$

where the primes indicate partial differentiation with respect to η and

$$\frac{\partial(f',f)}{\partial(\xi,\eta)}=\frac{\partial f'}{\partial\xi}f'-f''\frac{\partial f}{\partial\xi} \tag{15}$$

is the Jacobian.

The parameter Λ in equation (14) contains the injection velocity and is given by

$$\Lambda=\frac{Re}{n}\frac{V(\xi)}{U_\infty}[(n+1)\xi]^{n/(n+1)}. \tag{16}$$

The parameter Λ, which will be called the 'injection parameter' hereafter, is a function of ξ (i.e., x) only and its form depends on the injection distribution $V(\xi)$. Note that if $V(\xi)$ is negative, Λ will become the suction parameter.

The boundary conditions (3a,b,c) are transformed to

$$f'=-\frac{U_w}{U_\infty}=-\lambda, \quad f=0 \quad \text{at } \eta=0 \tag{17a,b}$$

$$f'=1 \quad \text{at } \eta=\infty \tag{17c}$$

where λ is called the plate velocity ratio parameter. The actual form of the transformed boundary condition (17b) is $\{f+(n+1)\xi(\partial f/\partial\xi)\}=0$. However, the definition of the stream function in equations (7a, b) essentially makes the flat plate a non-penetrable surface for which the boundary condition $f=0$ at $\eta=0$ is set and $\partial f/\partial\xi$ vanishes at the surface.

It is clear that when Λ is a constant, the right hand side of equation (14) vanishes and a similarity solution exists. This is possible only when there is no injection or when $V(\xi)/U_\infty\propto\xi^{-n/n+1}$. For any other injection distribution, a similarity solution does not exist.

Since Λ and ξ are functions of x only, there is a one-to-one correspondence between Λ and ξ. This suggests that a Merk–Chao series in which the solution is expanded in terms of derivatives of Λ can be used. The dimensionless stream function is written as

$$f(\xi,\eta,n)=f_0(\Lambda,\eta,n)+(n+1)\xi\frac{d\Lambda}{d\xi}f_1(\Lambda,\eta,n)+(n+1)^2\xi^2\frac{d^2\Lambda}{d\xi^2}f_2(\Lambda,\eta,n)+(n+1)^2\xi^2\left(\frac{d\Lambda}{d\xi}\right)^2 f_3(\Lambda,\eta,n)+\cdots. \tag{18}$$

Substituting equation (18) into equation (14) and collecting terms containing similar perturbation quantities, a set of sequential differential equations is generated.

The first equation representing local similarity is

$$f_0'''(f_0'')^{n-1}+(f_0-\Lambda)f_0''=0 \tag{19}$$

with the boundary conditions

$$f_0(\Lambda,0,n)=0, \quad f_0'(\Lambda,0,n)=-\lambda \tag{20a,b}$$

$$f_0'(\Lambda,\infty,n)=1. \tag{20c}$$

For the perturbation quantities

$$(n+1)\xi\frac{d\Lambda}{d\xi},(n+1)^2\xi^2\frac{d^2\Lambda}{d\xi^2} \quad \text{and} \quad (n+1)^2\xi^2\left(\frac{d\Lambda}{d\xi}\right)^2$$

the following higher-order equations are obtained:

$$(f_0'')^{n-1}f_1''' + (n-1)f_0'''(f_0''')^{n-2}f_1'' + (f_0-\Lambda)f_1'' - (n+1)f_0'f_1' + (n+2)f_0''f_1 = f_0'\frac{\partial f_0'}{\partial\Lambda} - f_0''\frac{\partial f_0}{\partial\Lambda} \quad (21)$$

$$(f_0'')^{n-1}f_2''' + (n-1)f_2'''(f_0'')^{n-2}f_2'' + (f_0-\Lambda)f_2'' - 2(n+1)f_0'f_2' + (2n+3)f_0''f_2 = f_0'f_1' - f_0''f_1 \quad (22)$$

$$(f_0'')^{n-1}f_3''' + (n-1)f_0'''(f_0'')^{n-2}f_3'' + (f_0-\Lambda)f_3'' - 2(n+1)f_0'f_3' + (2n+3)f_0''f_3 + (n-1)f_1'''(f_0'')^{n-2}f_1'' + \frac{(n-1)(n-2)}{2}f_0'''(f_0')^{n-3}(f_1'')^2 + (n+2)f_1f_1'' - (n+1)(f_1')^2 = f_0'\frac{\partial f_1'}{\partial\Lambda} - f_0''\frac{\partial f_1}{\partial\Lambda} + f_1'\frac{\partial f_0'}{\partial\Lambda} - f_1''\frac{\partial f_0}{\partial\Lambda} \quad (23)$$

with the associated boundary conditions:

$$f_i(\Lambda,0,n) = 0, \quad f_i'(\Lambda,0,n) = 0 \quad (24a,b)$$

$$f_i'(\Lambda,\infty,n) = 0 \quad \text{for } i = 1,2,3. \quad (24c)$$

At any given value of Λ, obtained at any streamwise location x, the above equations can be solved sequentially as ordinary differential equations. The f_is are universal functions to be solved once and for all for specific values of n, λ and Λ regardless of ξ or the form of the injection velocity distribution.

Since analytical solutions could not be found for these equations, they are solved numerically in this work. Even though the equations represent two point boundary value problems as the condition at $\eta = \infty$ must be satisfied at a finite value of η in practice, the equations are solved as initial value problems. A third condition at $\eta = 0$ is chosen by guessing a value for $f_i''(0)$ and is iteratively improved until the condition at $\eta = \infty$ is matched with sufficient accuracy. In every iteration an equation is integrated with the three initial conditions using a fourth-order Runge–Kutta method with step size control. Since f' reaches its value at $\eta = \infty$ asymptotically, the additional condition, $f''(\infty) = 0$, must also be satisfied. Accordingly, integration is carried out up to a point where $f''(\eta)$ is sufficiently close to zero. Then, using the Newton–Raphson method the value of the third initial condition is corrected depending on the value of $f_i'(\infty)$.

A general computer program was developed to solve all of the equations. While running the program, it was found that the universal functions converged rapidly. Therefore, only the first three universal functions are calculated. Although the velocity profiles can be generated using the program, the quantity of practical interest is the shear stress or friction coefficient at the wall, which can be calculated by knowing the values of $f_i''(0)$. The quantities $f_0''(0)$, $f_1''(0)$ and $f_2''(0)$ are tabulated for various values of n, λ and Λ. Seven values of n are selected for the calculation [15]. They are $n = 0.229$ (23.3% Illinois yellow clay in water), $n = 0.52$ (10% napalm in kerosene), $n = 0.716$ (0.67% CMC in water), $n = 1$ (Newtonian fluid), $n = 1.2$, 1.5 and 1.8 (ethylene oxide in sodium chloride solution). Three values, 0, 0.1 and 0.2, are chosen for λ.

In order to ensure that a flow with suction or injection at the wall satisfies the boundary layer equations, it is necessary to limit the velocity $V_w(x)$ at the wall to a magnitude on the order of $U_\infty\, Re^{-1/n+1}$ [16]. Only when the velocity is of such small magnitude is it possible to neglect the loss of mass, or 'sink effect', on the external potential flow. In other words, the potential flow may be assumed to be unaffected by such suction or injection. Due to this requirement, the realistic values of the injection parameter, which is given by

$$\Lambda = \frac{V_w(x)}{U_\infty}Re^{1/(n+1)}\left((n+1)\frac{x}{L}\right)^{\frac{n}{n+1}}\left(\frac{1}{n}\right)^{\frac{1}{n+1}} \quad (25)$$

are limited within a certain range. For this reason, the magnitude of Λ is limited to 2.5 in this study.

The analysis done by Vajravelu and Mohapatra [14] for the Newtonian case shows that there exists a critical value of injection at a given value of λ, above which the boundary layer structure collapses and the boundary layer approximations are no longer valid. The critical value of injection is a strong function of λ. This is also true for the present analysis. Above a certain value of Λ, the f_i equations are not solvable. In this study it was found that this critical value of injection depends not only on the value of λ but also on the value of n. At constant n, the critical value decreases with λ. At constant λ, the critical value also decreases with n but this dependence is less than in the former case. This critical value is the maximum value of Λ for the case of injection up to which the results are tabulated. Since no such critical value exists for suction, the results are tabulated up to the maximum value selected, which is -2.5.

In Tables 1 and 2, the universal wall derivatives are presented for $n = 0.229$ and 1.2, respectively. Results for other values of n and Λ can be found in [17]. To verify the numerical solution procedure and the computer program, some of the present results are compared with those reported in previous works. For the case of a stationary plate with no injection, i.e., when $\Lambda = 0$, the f_0 equation is the same as the f_0 equation presented by Kim et al. [19]. The values of $f_0''(0)$ for both studies agree well for all values of n.

Table 1
Numerical results of $f_0''(0)$ for $n = 0.229$

λ	Λ	$f_0''(0)$	$f_1''(0)$	$f_2''(0)$
0	−2.50	1.24631681	0.09247901	−0.01628465
	−1.50	0.57657097	0.05758343	−0.01076963
	−0.75	0.30809930	0.03798774	−0.00745771
	−0.25	0.19860355	0.02787707	−0.00565525
	0.00	0.15855324	0.02364322	−0.00487497
	0.50	0.10009347	0.01667117	−0.00354826
	1.00	0.06257607	0.01145862	−0.00251328
	2.00	0.02416298	0.00507152	−0.00117257
	2.50	0.01506083	0.00329449	−0.00077861
0.1	−2.50	1.55682702	0.10845347	−0.01926821
	−1.50	0.67680618	0.06310968	−0.01198972
	−0.75	0.33469426	0.03833815	−0.00773178
	−0.25	0.20085890	0.02589397	−0.00548129
	0.00	0.15341734	0.02077488	−0.00453033
	0.50	0.08654745	0.01245696	−0.00296559
	1.00	0.04602085	0.00614267	−0.00184862
0.2	−2.50	1.93904003	0.12081976	−0.02222974
	−1.50	0.78007952	0.06180001	−0.01280486
	−0.75	0.35155495	0.02890442	−0.00753559
	−0.25	0.19011290	0.01020752	−0.00531213
	0.00	0.13428205	−0.00007489	−0.00536205
	0.30	0.08310751	−0.02055867	−0.01417871

Table 2
Numerical results of $f_i''(0)$ for $n = 1.2$

λ	Λ	$f_0''(0)$	$f_1''(0)$	$f_2''(0)$
0	−2.50	2.61499127	0.02354229	−0.00139398
	−1.50	1.80412405	0.03938741	−0.00322018
	−0.75	1.17434241	0.06072315	−0.00629977
	−0.25	0.74765469	0.08233622	−0.00994112
	0.00	0.53506307	0.09608013	−0.01249157
	0.20	0.36748990	0.10873447	−0.01500696
	0.40	0.20486389	0.12319196	−0.01811544
	0.50	0.12685385	0.13152161	−0.02004885
0.1	−2.50	2.81817490	0.02282438	−0.00135947
	−1.50	1.93416065	0.03810219	−0.00313795
	−0.75	1.24282593	0.05845945	−0.00612806
	−0.25	0.76801572	0.07844337	−0.00963737
	0.00	0.52631749	0.09002073	−0.01205633
	0.20	0.32922100	0.09679003	−0.01436231
0.2	−2.50	3.01536929	0.02136170	−0.00130354
	−1.50	2.05769371	0.03520271	−0.00299523
	−0.75	1.30265479	0.05219952	−0.00578755
	−0.25	0.77437284	0.06272605	−0.00893767
	0.00	0.49484629	0.04872731	−0.01170724
	0.10	0.37480220	0.00499563	−0.01833166

4. Solution of the energy equation

For the heat transfer analysis, the same coordinate transformations as used for the analysis of the momentum transfer are again used. A dimensionless temperature $\theta(\xi,\eta)$ is defined in terms of the transformed coordinates as

$$\theta(\xi,\eta) = \frac{T-T_w}{T_\infty - T_w}. \tag{26}$$

The energy equation (5) is then transformed to

$$\theta'' + \Lambda_1 (f-\Lambda)\theta' = \Lambda_1 (n+1)\xi \frac{\partial(\theta,f)}{\partial(\xi,\eta)} \tag{27}$$

where the primes indicate differentiation with respect to η and

$$\frac{\partial(\theta,f)}{\partial(\xi,\eta)} = \frac{\partial\theta}{\partial\xi}\frac{\partial f}{\partial\eta} - \frac{\partial\theta}{\partial\eta}\frac{\partial f}{\partial\xi} \tag{28}$$

is the Jacobian.

The parameter Λ_1 is a function of ξ except when $n = 1$, and is given by

$$\Lambda_1 = n\frac{\mu_0}{\rho\alpha}\left(\frac{U_\infty}{L}\right)^{n-1}$$

$$[(n+1)\xi]^{(1-n)/(1+n)} = n\,Pr\left[n(n+1)\left(\frac{x}{L}\right)\right]^{\frac{1-n}{1+n}} \tag{29}$$

where Pr is the generalized Prandtl number defined as

$$Pr = \frac{1}{\alpha} U_\infty L\, Re^{2/(n+1)}. \tag{30}$$

From the expression for Λ_1, one can observe that it will be on the same order of magnitude as the generalized Prandtl number. In fact, when $n = 1$, Λ_1 is equal to the regular Prandtl number, $\hat{C}_p\mu/k$. The value of Λ_1 determines the relative thicknesses of the momentum and thermal boundary layers. When Λ_1 is large, the thermal boundary layer is small compared to the momentum boundary layer.

Since equation (27) contains two independent parameters, Λ and Λ_1, the Merk–Chao series is expanded in these two parameters. The dimensionless temperature θ is expanded as follows:

$$\begin{aligned}\theta(\xi,\eta,n) = {} & \theta_0 + (n+1)\xi\frac{d\Lambda}{d\xi}\theta_1 + (n+1)\xi\frac{d\Lambda_1}{d\xi}\theta_2 \\ & + (n+1)^2\xi^2\frac{d^2\Lambda}{d\xi^2}\theta_3 \quad + (n+1)^2\xi^2\frac{d^2\Lambda_1}{d\xi^2}\theta_4 \\ & + (n+1)^2\xi^2\left(\frac{d\Lambda}{d\xi}\right)^2\theta_5 + (n+1)^2\xi^2\left(\frac{d\Lambda_1}{d\xi}\right)^2\theta_6 \\ & + (n+1)^2\xi^2\frac{d\Lambda}{d\xi}\frac{d\Lambda_1}{d\xi}\theta_7 + \cdots.\end{aligned} \tag{31}$$

When equation (18) and (31) are substituted into (27) and terms containing similar perturbation quantities are

collected, the following set of sequential differential equations is obtained:

$$\theta_0'' + \Lambda_1(f_0 - \Lambda)\theta_0' = 0 \tag{32}$$

$$\theta_1'' + \Lambda_1(f_0 - \Lambda)\theta_1' - \Lambda_1(n+1)f_0'\theta_1 + \Lambda_1(n+2)f_1\theta_0' = \Lambda_1\left(\frac{\partial\theta_0}{\partial\Lambda}f_1' - \theta_0'\frac{\partial f_0}{\partial\Lambda}\right) \tag{33}$$

$$\theta_2'' + \Lambda_1(f_0 - \Lambda)\theta_2' - \Lambda_1(n+1)f_0'\theta_2 = \Lambda_1\frac{\partial\theta_0}{\partial\Lambda_1}f_0' \tag{34}$$

$$\theta_3'' + \Lambda_1(f_0 - \Lambda)\theta_3' - 2\Lambda_1(n+1)f_0'\theta_3 + \Lambda_1(2n+3)f_2\theta_0' = \Lambda_1(\theta_1 f_0' - \theta_0' f_1) \tag{35}$$

$$\theta_4'' + \Lambda_1(f_0 - \Lambda)\theta_4' - 2\Lambda_1(n+1)f_0'\theta_4 - \Lambda_1 f_0'\theta_2 = 0. \tag{36}$$

The associated boundary conditions are

$$\theta_0(0) = 0, \quad \theta_0(\infty) = 1 \tag{37a,b}$$

$$\theta_i(0) = 0, \quad \theta_i(\infty) = 0 \quad \text{for } i = 1, 2, 3, 4, \cdots. \tag{38a,b}$$

It should be noted that when $n = 1$, Λ_1 is a constant and the higher order universal functions $\theta_2, \theta_4, \theta_6, \theta_7, \ldots$, have no relevance. Similarly when there is no injection or when Λ is not a function of ξ, the quantities θ_1, θ_3, θ_5, $\theta_7, \ldots$, have no relevance.

All of the above equations are linear second-order ordinary differential equations which can be solved sequentially for the universal functions θ_is. As is done for the f_i equations, these are solved as initial value problems using a fourth-order Runge–Kutta method for integration and the Newton–Raphson method for improving the unknown initial condition. The quantity of interest is the heat flux at the surface, which can be obtained from the values of $\theta_i'(0)$. In this case, the universal functions depend on n, λ, Λ and Λ_1. Three values, 0.52, 1, and 1.2 are selected for n. The values of λ and Λ are chosen as before. For a given fluid, the parameter Λ_1 depends on the Prandtl number and the location along the surface. To obtain meaningful values for Λ_1, two values, 0.7 and 7, are chosen for Pr, one representing gases and the other representing liquids. Three values, 0.1, 0.5 and 1, are chosen for x/L except for Newtonian fluids in which case the parameter Λ_1 is equal to the Prandtl number and has no x/L dependency.

In Table 3 the numerical results of $\theta_i'(0)$ are presented for $n = 0.52$ and $\Lambda_1 = 1.633$. In Table 4, these results are given for $n = 1.2$ and $\Lambda_1 = 0.819$. The results for more extensive values of n and Λ_1 are given in [17].

5. Significant momentum and heat transfer quantities

Once the universal velocity and temperature functions are calculated, quantities such as the local friction coefficient and the Nusselt number can readily be calculated. The only other information needed is the injection distribution at the plate surface.

The shear stress exerted by the fluid on the plate is given by

$$\tau_w = \tau_{yx}|_{y=0} = \mu_0\left(\frac{\partial u}{\partial y}\right)^n\bigg|_{y=0}. \tag{39}$$

Defining the local friction coefficient as $c_f = (\tau_w/\rho U_\infty^2/2)$ and writing it in a form analogous to that for a Newtonian fluid gives

$$\frac{1}{2}c_f\,Re^{1/(n+1)} = \left[n(n+1)\frac{x}{L}\right]^{\frac{-1}{n+1}}\left\{f_0''(0) + (n+1)\xi\frac{d\Lambda}{d\xi}f_1'(0) + (n+1)^2\xi^2\frac{d^2\Lambda}{d\xi^2}f_2''(0) + \cdots\right\}^n. \tag{40}$$

The heat flux at the wall is given by

$$q_w = -k\frac{\partial T}{\partial y}\bigg|_{y=0}. \tag{41}$$

The Nusselt number is expressed as

$$\begin{aligned} Nu\,Re^{(-1)/(n+1)} &= \frac{hL}{k}Re^{(-1)/(n+1)} = L\frac{\partial\theta}{\partial y}\bigg|_{y=0}Re^{(-1)/(n+1)} \\ &= \left[n(n+1)\frac{x}{L}\right]^{\frac{-1}{1+n}}\left\{\theta_0'(0) + (n+1)\xi\frac{d\Lambda}{d\xi}\theta_1'(0) + (n+1)\xi\frac{d\Lambda_1}{d\xi}\theta_2'(0) + (n+1)^2\xi^2\frac{d^2\Lambda}{d\xi^2}\theta_3'(0) + (n+1)^2\xi^2\frac{d^2\Lambda_1}{d\xi^2}\theta_4'(0) + \cdots\right\}. \end{aligned} \tag{42}$$

6. Application

In this section it is demonstrated how the general solutions can be applied for a special case. The simplest case for this problem is when the injection velocity takes the form $V(\xi)/U_\infty = K\xi^{-[n/(n+1)]}$, where K is a constant. In this case, the injection parameter Λ becomes constant and the similarity solution applies for the velocity field, i.e., only the first term in equation (18) is required. However, no similarity solution exists for the temperature field even in this case. The similarity solution has been studied for the velocity field by Vajravelu and Mohapatra [14] for a Newtonian fluid and by Akcay and Yukselen [18] for a non-Newtonian fluid. The most common and easiest laboratory simulation is for a constant injection along the length of the plate. For this case, the similarity solution cannot be applied to either the velocity or the temperature field. For this case

Table 3
Numerical results of $\theta_i'(0)$ for $n = 0.520$ and $\Lambda_1 = 1.633$ (Λ_1 corresponding to $Pr = 7$ and $x/L = 0.1$)

λ	Λ	$\theta_0'(0)$	$\theta_1'(0) \times 10$	$\theta_2'(0) \times 10$	$\theta_3'(0) \times 10^2$	$\theta_4'(0) \times 10^2$
0	−2.50	4.196733	0.288444	−0.813837	−0.096000	0.553219
	−1.50	2.606704	0.567390	−0.874152	−0.413789	0.909087
	−0.75	1.460555	1.035030	−0.791905	−1.237035	1.169097
	−0.25	0.767777	1.472697	−0.537995	−2.324261	1.020001
	0.00	0.472629	1.591172	−0.326373	−2.820403	0.718527
	0.50	0.086387	0.944832	0.027195	−1.967108	0.006055
	1.00	0.001676	0.051903	0.007326	−0.113209	−0.011877
0.1	−2.50	4.176176	0.214521	−0.762132	−0.051735	0.519820
	−1.50	2.572396	0.428191	−0.804618	−0.292827	0.844217
	−0.75	1.404828	0.818208	−0.713590	−0.995903	1.072692
	−0.25	0.690127	1.218885	−0.454049	−2.027693	0.885980
	0.00	0.386587	1.309695	−0.239219	−2.482515	0.549682
	0.50	0.032523	0.423613	0.026681	−1.009904	−0.035763
	0.75	0.001400	0.020844	0.003201	−0.103072	−0.006640
0.2	−2.50	4.155839	0.135010	−0.710982	−0.013179	0.488983
	−1.50	4.108080	0.130026	−0.382348	−0.021037	0.308521
	−0.75	1.344342	0.487421	−0.625440	−0.758872	0.973874
	−0.25	0.598383	0.640949	−0.355404	−1.783894	0.732799
	0.00	0.280330	0.413156	−0.142389	−2.480133	0.345601
	0.20	0.093002	−0.377028	−0.018228	−4.353858	0.035946

Table 4
Numerical results of $\theta_i'(0)$ for $n = 1.2$ and $\Lambda_1 = 0.819$ (Λ_1 corresponding to $Pr = 0.7$ and $x/L = 0.5$)

λ	Λ	$\theta_0'(0)$	$\theta_1'(0) \times 10$	$\theta_2'(0) \times 10$	$\theta_3'(0) \times 10^2$	$\theta_4'(0) \times 10^2$
0	−2.50	2.226195	0.334889	−1.613782	−0.277005	1.502401
	−1.50	1.474776	0.460740	−1.485074	−0.464985	1.746394
	−0.75	0.942275	0.573140	−1.152190	−0.660677	1.609376
	−0.25	0.611181	0.652501	−0.777634	−0.816715	1.227319
	0.00	0.455098	0.696898	−0.548824	−0.909867	0.933055
	0.10	0.394600	0.717902	−0.452203	−0.954237	0.797694
	0.30	0.276661	0.776555	−0.256608	−1.074618	0.504186
	0.50	0.160405	0.921628	−0.071684	−1.347679	0.198231
0.1	−2.50	2.210826	0.307589	−1.568367	−0.257332	1.467759
	−1.50	1.454309	0.420922	−1.437498	−0.429557	1.701817
	−0.75	0.915257	0.515943	−1.097334	−0.601154	1.545541
	−0.25	0.576407	0.571870	−0.711231	−0.725968	1.135841
	0.00	0.413598	0.590624	−0.472391	−0.789931	0.817188
	0.10	0.349076	0.592573	−0.370664	−0.817161	0.668926
	0.30	0.216417	0.513436	−0.161181	−0.897591	0.337626
0.2	−2.50	2.195121	0.277952	−1.521474	−0.238193	1.432944
	−1.50	1.433170	0.374623	−1.387694	−0.393762	1.655927
	−0.75	0.886670	0.439919	−1.039636	−0.537841	1.479560
	0.00	0.364072	0.275282	−0.384704	−0.684981	0.681166
	0.10	0.290915	−0.033499	−0.273163	−1.047211	0.508937

$$V_w(x) = v_0 \tag{43}$$

$$\Lambda = \frac{Re}{n}\frac{v_0}{U_\infty}[(n+1)\xi]^{n/(n+1)}. \tag{44}$$

The parameter Λ_1 is independent of the injection distribution

$$\Lambda_1 = n\frac{\mu_0}{\rho\alpha}\left(\frac{U_\infty}{L}\right)^{n-1}[(n+1)\xi]^{(1-n)/(1+n)} \tag{45}$$

and the coefficients of the universal functions in the Merk–Chao series are

$$(n+1)\xi\frac{d\Lambda}{d\xi} = n\Lambda \tag{46}$$

$$(n+1)^2\xi^2\frac{d^2\Lambda}{d\xi^2} = -n\Lambda \tag{47}$$

$$(n+1)\xi\frac{d\Lambda_1}{d\xi} = (1-n)\Lambda_1 \tag{48}$$

and

$$(n+1)^2\xi^2\frac{d^2\Lambda_1}{d\xi^2} = -2n(1-n)\Lambda_1. \tag{49}$$

The dimensionless axial velocity profile is

$$f' = f'_0 + n\Lambda f'_1 - n\Lambda f'_2 + \cdots. \tag{50}$$

One can find the local friction coefficient by knowing the values of $f''_i(0)$:

$$\frac{1}{2}c_f Re^{1/(n+1)} = \left[n(n+1)\frac{x}{L}\right]^{\frac{-1}{n+1}}\{f''_0(0) + n\Lambda f'_1(0) - n\Lambda f''_2(0) + \cdots\}^n. \tag{51}$$

There is an order of magnitude reduction between the successive f_i values. As the values of Λ are limited within a certain range, the magnitude of the coefficients is not large enough to alter this reduction significantly. Hence the series converges rapidly and the first three terms give an accurate solution.

The dimensionless temperature is

$$\theta = \theta_0 + n\Lambda\theta_1 + (1-n)\Lambda_1\theta_2 - n\Lambda\theta_3 - 2n(1-n)\Lambda_1\theta_4 + \cdots \tag{52}$$

and the Nusselt number can be calculated by knowing the values of $\theta'_i(0)$:

$$Nu\,Re^{(-1)/(n+1)} = \left[n(n+1)\frac{x}{L}\right]^{\frac{-1}{1+n}}\{\theta'_0(0) + n\Lambda\theta'_1(0) + (1-n)\Lambda_1\theta'_2(0) - n\Lambda\theta'_3(0) - 2n(1-n)\theta'_4(0) + \cdots\}. \tag{53}$$

In this case, the successive odd numbered and even numbered terms decrease at a much faster rate than the terms in the momentum solution. In Table 5, the quantities $\frac{1}{2}c_f Re^{1/(n+1)}$ and $Nu\,Re^{(-1)/(n+1)}$ are given for few cases when there is constant injection/suction.

The convergence of equations (51) and (53) is very good for the parameter range studied. For example, for $n = 0.229$, $\lambda = 0$, and $\Lambda = 0.75$, the magnitude of the first term in equation (51) is 96.4% of the value of the whole series. A more detailed study of the convergence of these series is available in [17].

The dimensionless velocity and temperature profiles given by equations (50) and (52), respectively, can be used to observe the effect of various parameters on the behavior of the boundary layer. The thickness of the momentum boundary layer for fixed λ and Λ is largely determined by the power-law constant n, which determines by equation (4) how fast viscous momentum is transferred through the fluid layers in the boundary layer. The momentum boundary layer thickness decreases significantly with increasing n, and, conversely, the velocity gradient at the wall increases as can be seen from the values in Tables 1 and 2. The value of n also influences the thermal boundary layer thickness in the same manner, but to a lesser extent. The thermal boundary layer thickness primarily depends on the magnitude of the parameter Λ_1, which contains the Prandtl number. If Λ_1 is large, the thermal boundary layer thickness is going to be small and the temperature gradient at the wall is large. At constant Λ_1 or Pr values, this thickness decreases with n. These effects have been mentioned by Kim et al. [19] and more detail is given in [17].

Injecting fluid into the boundary layer increases both the momentum and thermal boundary layer thicknesses as shown in Figs 2 and 3, respectively. As a consequence of this, the velocity and temperature gradients at the surface decrease, resulting in lower friction coefficients and Nusselt numbers at the wall, as listed in Table 5. As is also shown in these figures and table, suction has exactly the opposite effect. Increasing the suction increases the velocity and temperature gradients at the wall by decreasing the momentum and thermal boundary layer thicknesses. This is true for all values of n and λ studied in [17].

The effect of the plate velocity ratio parameter, λ, is somewhat different. When there is injection, increasing λ at a constant value of Λ increases the momentum boundary layer thickness, which decreases the wall velocity gradient and results in a lower friction coefficient. This is also true when $\Lambda = 0$. When there is suction, increasing λ at a constant value of Λ has the opposite effect. Thus, when the plate is moved with a greater speed opposite to the mainstream, the effects of suction and injection are enhanced. At a given n and λ, the decrease/increase in wall shear stress with respect to Λ for the case of injection/suction is almost constant over the entire range of Λ values presented [17]. This decrease/increase is larger at higher values of λ.

Table 5
Numerical results of $\frac{1}{2}c_f Re^{1/(n+1)}$ and $Nu\,Re^{(-1)/(n+1)}$ for the case of constant injection/suction

n	λ	Λ	x/L	$\frac{1}{2}c_f Re^{1/(n+1)}$	Λ_1	$Nu\,Re^{(-1)/(n+1)}$
0.52		−0.5	0.966	0.832305	0.338	0.444059
	0	0	0.966	0.618177	0.338	0.304191
		0.5	0.966	0.428789	0.338	0.184882
		−0.5	0.966	0.858622	0.338	0.423571
	0.1	0	0.966	0.610068	0.338	0.272947
		0.5	0.966	0.381134	0.338	0.136256
1		−0.5	0.707	0.721419	0.7	0.553798
	0	0	0.707	0.394885	0.7	0.348057
		0.5	0.707	0.124853	0.7	0.174672
		−0.5	0.707	0.759257	0.7	0.533142
	0.1	0	0.707	0.387694	0.7	0.315028
		0.4	0.791	0.114731	0.7	0.131875
1.2		−0.5	0.634	0.754565	0.948	0.651438
	0	0	0.634	0.373579	0.948	0.483491
		0.5	0.634	0.066414	0.948	0.176285
		−0.5	0.634	0.797659	0.948	0.627534
	0.1	0	0.634	0.366264	0.948	0.351970
		0.3	0.838	0.117562	0.948	0.168801

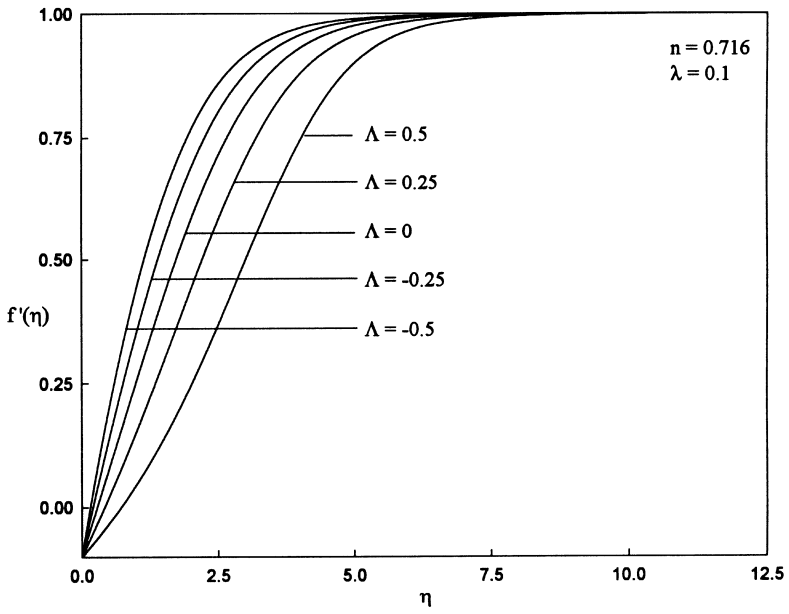

Fig. 2. Effect of injection/suction on dimensionless velocity profiles for $n = 0.716$ and $\lambda = 0.1$.

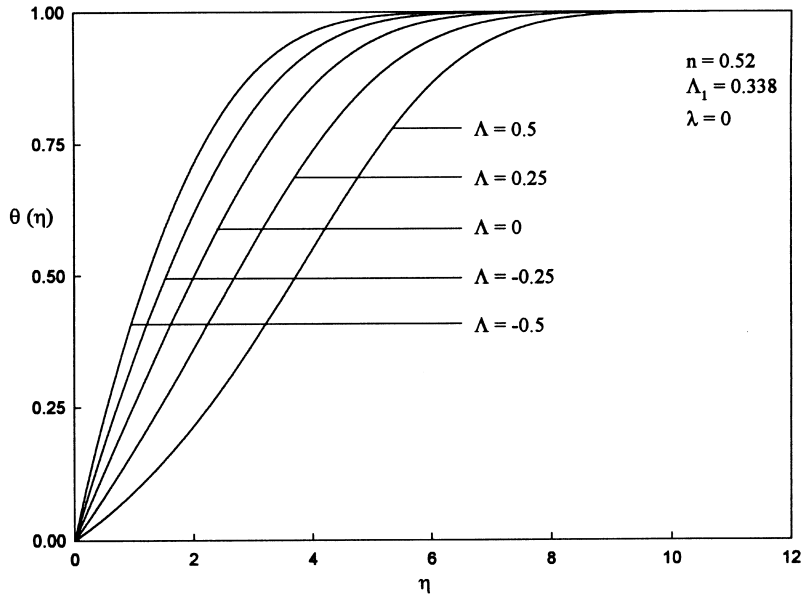

Fig. 3. Effect of injection/suction on dimensionless temperature profiles for $n = 0.52$, $\lambda = 0$ and $\Lambda_1 = 0.338$.

It is interesting to note that the effect of the plate velocity parameter λ on the heat transfer is different from its effect on the momentum transfer. Increasing λ at a constant value of Λ decreases the temperature gradient and the Nusselt number at the surface in both cases of suction and injection. Figure 4 shows this effect of plate velocity on the dimensionless temperature profiles when injection is present. For the case of constant suction, a similar trend of the temperature profile is observed [17]. Table 5 shows the same behavior for the Nusselt number.

The critical value of Λ, which is the maximum value of the injection parameter, is also a strong function of the power-law constant n, and the plate velocity ratio, λ. At constant n, the critical value decreases with λ. At constant λ, the critical value decreases with n but this dependence is less than that in the former case [17].

7. Conclusions

The momentum and heat transfer in the laminar non-Newtonian boundary layer of a moving flat plate with

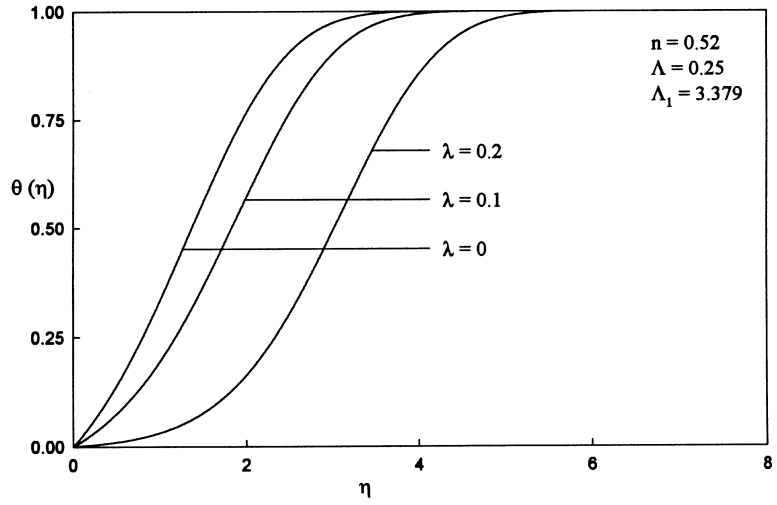

Fig. 4. Effect of plate velocity on dimensionless temperature profiles for $n = 0.52$ and $\Lambda_1 = 3.379$ with injection present.

arbitrary injection/suction at the surface have been analyzed. The main objective of this study, that of obtaining boundary layer solutions for any form of the fluid injection/suction distribution along the surface, is achieved by absorbing the injection/suction velocity into the governing equations. Then, by using the Merk–Chao series expansion, those equations are decomposed into an infinite sequence of ordinary differential equations. The solutions to these equations are expressible in terms of universal functions, which are independent of the injection/suction velocity distribution at the surface. This is a significant improvement over the previous similarity solutions, which are applicable only for a particular form of the injection distribution.

The present method of obtaining the solution for a particular injection/suction profile is illustrated for the case of constant velocity at the plate surface. For this case, the convergence of the Merk–Chao series is excellent. The effects of the injection parameter and the plate velocity ratio on the velocity and temperature profiles and on the friction coefficient and Nusselt number at the wall are discussed. Increasing the value of the injection parameter reduces the velocity and the temperature gradients at the wall and decreases the friction coefficient and the Nusselt number significantly. Suction has exactly the opposite effects. Increasing the plate velocity ratio decreases the friction coefficient and the Nusselt number at the wall when injection is present. With suction present, increasing the plate velocity ratio increases the friction coefficient but decreases the Nusselt number.

The requirement that the injection velocity be small compared to the mainstream velocity in order to validate the boundary layer assumptions limits the use of the present solution procedure to such cases where the injection parameter is below a certain critical value. The critical values found with the present numerical procedure are in close agreement with those reported in previous works. This critical value decreases as the power-law constant increases. Also, at a given value of the power-law constant, the critical value decreases drastically with the plate velocity ratio.

References

[1] W.R. Schowalter, The application of boundary layer theory to power-law pseudoplastic fluid: similar solutions, American Inst. of Chemical Engs J. 6 (1960) 24–28.

[2] A. Acrivos, M.J. Shah, E.E. Petersen, Momentum and heat transfer in laminar boundary layer flows of non-Newtonian fluids past external surfaces, American Inst. of Chemical Engs J. 6 (1960) 312–318.

[3] S.Y. Lee, W.F. Ames, Similarity solutions for non-Newtonian fluids, American Inst. of Chemical Engs J. 12 (1966) 700–708.

[4] B.M. Berkovskii, A class of self-similar boundary layer problems for rheological power-law fluids, International Chemical Engineering 6 (2) (1966) 187–201.

[5] A.G. Hansen, R.Y. Na, Similarity solutions of laminar incompressible boundary layer equations of non-Newtonian fluids, Transactions of the ASME, Journal of Basic Engineering 40 (1968) 71–74.

[6] S. Thurston, R.D. Jones, Experimental model studies of non-Newtonian soluble coatings for drag reduction, AIIA Paper 64-466, Washington, D.C., 1964.

[7] E.R. Thompson, W.T. Snyder, Drag reduction of a non-Newtonian fluid by fluid injection at the wall, J. of Hydronautics 2 (1968) 177–180.

[8] E.R. Thompson, W.T. Snyder, Laminar boundary layer flows of Newtonian fluids with non-Newtonian fluid injections, J. of Hydronautics 4 (1970) 86–91.

[9] K.H. Kim, A.H. Eraslan, Non-Newtonian stagnation flow with mass injection, J. of Hydronautics 2 (1968) 121–123.

[10] K.H. Kim, A.H. Eraslan, Flow of a non-Newtonian fluid past wedges with wall mass injection, J. of Hydronautics 3 (1969) 157–159.

[11] C.Y. Liu, Asymptotic suction flow of power-law fluids, J. of Hydronautics 7 (1973) 135–136.

[12] J.B. Klemp, A. Acrivos, A method for integrating the boundary layer equations through a region of reverse flow, J. Fluid Mech. 53 (1972) 177–191.

[13] M.Y. Hussaini, W.D. Lakin, Existence and uniqueness of similarity solution of a boundary layer problem, Quart. J. Mech. Appl. Math. 39 (1986) 15–24.

[14] K. Vajravelu, R.N. Mohapatra, On fluid dynamic drag reduction in some boundary layer flows, Acta Mechanica 81 (1990) 59–68.

[15] A.B. Metzner, Advances in Chemical Engineering, vol. 1, Academic Press, New York, 1956.

[16] H. Schlichting, Boundary Layer Theory, 7th ed., McGraw-Hill, New York, 1979.

[17] J.H. Rao, Momentum and thermal boundary layer analyses of power-law fluid over a moving flat plate with arbitrary injection at the surface, Masters' Thesis, The University of Toledo, Toledo, Ohio, 1997.

[18] M. Akcay, M.A. Yukselen, On drag reduction of a non-Newtonian fluid by fluid injection at the moving wall, private communication to D.R. Jeng at the University of Toledo, Toledo, OH.

[19] H.W. Kim, D.R. Jeng, K.J. DeWitt, Momentum and heat transfer in power-law fluid flow over two-dimensional or axisymmetric bodies, Int. J. of Heat Mass Transfer 26 (2) (1983) 245–259.